# XAS Study of Au Supported on $TiO_2$: Influence of Oxidation State and Particle Size on Catalytic Activity

**Viviane Schwartz,* David R. Mullins, Wenfu Yan, Bei Chen, Sheng Dai, and Steven H. Overbury**

*Chemical Sciences Division, Oak Ridge National Laboratory, Oak Ridge, Tennessee 37831-6201*

*Received: May 4, 2004; In Final Form: July 26, 2004*

The effect of synthesis and reaction conditions on the structure and activity of Au clusters supported on nanocrystalline and mesoporous $TiO_2$ was investigated. X-ray absorption spectroscopy was applied to correlate the particle size and the oxidation state with several parameters, such as pH of the precursor solution, Au loading, pretreatment, and support structure. The study using mesoporous $TiO_2$ as the support shows that lower Au loadings resulted in bigger Au aggregates with lower reducibility. The high activity state for Au supported in different allotropic forms of $TiO_2$ corresponds to Au in a fully reduced state. Furthermore, once reduced, no reoxidation occurs under reaction conditions, even after flowing air at higher temperatures (150 and 300 °C). Therefore, our results indicate that oxidized Au is not necessary for high activity. The activity decreased with particle growth, and, compared to the other allotropic $TiO_2$, Au on brookite exhibited no significant particle agglomeration and was the most active catalyst after treatment at 300 °C.

## Introduction

In recent years, catalysis by gold has received increasing attention since the discovery that small supported Au clusters exhibit extraordinarily high activity in many reactions, and, in particular, in CO oxidation at low temperatures.[1,2] The relationship between the high activity and the particle size has been clearly demonstrated. However, little is known about the factors that control this remarkable result and about the nature of the active sites. For instance, there is still a debate regarding the oxidation state of Au under reaction conditions. It has been suggested that small Au metal particles are responsible for the high activity for CO oxidation,[3] that cationic and reduced Au are present simultaneously during steady-state CO oxidation in other cases,[4,5,6,7,8,9] and that cationic Au species are the active phase for the water-gas shift reaction.[10]

It is generally accepted that the Au particle structure and the consequent catalytic properties depend on the support used, the Au loading, the synthesis method, and the pretreatment conditions. Among various supports, reducible oxides such as $TiO_2$ are among the most popular due to the expected strong metal−support interaction phenomena. Our goal was to vary many of these factors and characterize the gold supported on titania during the preparation and the working state. The catalysts under scrutiny were Au supported on different allotropic nanocrystalline forms of titania and on mesoporous titania material. Titania provides a good test, since the three crystalline structure types can be synthesized. This allows the examination of how the porosity, crystallite morphology, structure, and concentration of surface defects on the support structure may affect the size and morphology of the deposited Au catalyst's particles. X-ray absorption spectroscopy (XAS) was used to characterize the catalysts. The oxidation state was determined by X-ray absorption near-edge structure (XANES), whereas the determination of the neighboring atoms and their distance were obtained by extended X-ray absorption fine structure (EXAFS).

* To whom correspondence should be addressed: E-mail: schwartzv@ornl.gov. Tel: (865)576-6749. Oak Ridge National Laboratory, Chemical Sciences Division, P.O. Box 2008, MS-6201, Oak Ridge, TN 37831-6201.

## Experimental Section

**Sample Preparation.** Three sets of Au catalysts supported on $TiO_2$ were prepared to cover the scope of this work.

*Au on Nanocrystalline $TiO_2$ Prepared from Solutions with Variable pH.* A series of Au catalysts was prepared using commercially available $TiO_2$ supports (DeGussa P-25). The introduction of gold precursors on the $TiO_2$ support was achieved via a deposition−precipitation (D−P) method as follows. First, a solution of hydrogen tetrachloroaurate (III) trihydrate ($HAuCl_4 \cdot 3H_2O$, 99.9+%, Aldrich) was made by dissolving 3.0 g into 500 mL deionized water. Then, 50-g aliquots were adjusted to a pH of 2, 4, 6, 8, 10, or 11 with vigorous stirring, using a solution of 1.0 M KOH at room temperature. After pH adjustment, the solution was heated at 60 °C in a water bath. Next, 1.0 g $TiO_2$ powder was added. The resulting mixture was continuously stirred for 2 h. Finally, the precipitates were separated by centrifugation, then washed three times with deionized water and once with ethanol. The product was dried at 40 °C in air overnight to obtain the "as-synthesized" catalyst. Based upon the synthesis stoichiometry, if all Au adsorbs, the Au loading would be 13 wt %.

*Au on Mesoporous $TiO_2$ with Variable Loading.* The mesoporous titania support was synthesized according to a previously published approach.[11] In a typical preparation, 4.18 g titanium(IV) tetraethoxide was dissolved in 2.7 mL concentrated hydrochloric acid at room temperature under vigorous stirring. After 10−15 min, a solution of 1.0 g surfactant (triblock copolymer P123) dissolved in 12 mL dry ethanol was added. The solutions were subsequently aged with stirring at room temperature for about 30 min, poured into a glass Petri dish, and dried. After 2 days, the dried material was calcined (ramp to 180 °C at 2 °C/min, hold for 4 h, ramp to 315 °C at 2 °C/

10.1021/jp048076v CCC: $27.50 
Published on Web 09/04/2004

min, hold for 15 h) to remove the block copolymer species. After calcination, BET indicated good pore structure with a surface area of 178 $m^2/g$ (BET multipoint). The most probable pore size was 5.5 nm and the cumulative pore volume was 0.22 $cm^3/g$. The Au was introduced by adding variable amounts of hydrogen tetrachloroaurate (III) trihydrate to 50 mL water, adjusting the pH to7 by adding KOH with vigorous stirring, and then adding 0.8 g mesoporous titania. The resulting mixture was stirred for 4 h, filtered, washed with distilled water several times, and dried at 60 °C. The precursors were finally calcined in air at 200 °C for 3 h. Three Au sample loadings of 2.5, 5, and 10 wt % were prepared, based upon synthesis stoichiometry.

*Au on Different Allotropic Forms of Nanocrystalline $TiO_2$.* $TiO_2$ in the anatase, brookite, and rutile structural forms was prepared as described previously.[12] Basically, anatase and rutile were obtained in high purity by sonication synthesis using titanium (IV) tetra *iso*-propoxide and $TiCl_4$ precursors, respectively.[13] Brookite was obtained by hydrothermal synthesis using a $TiCl_4$ precursor.[14] The Au was introduced by D−P at a pH of 9.8−10.0 and the sample was dried at 50 °C in air overnight to yield the as-synthesized sample. The $TiO_2$ surface area and Au loading varied between samples. Based upon the synthesis stoichiometry, if all Au adsorbs, the Au loading would be 13 wt % in each case. According to analysis by ICP, the Au loadings were 13.7, 12.6, and 3.3 for the rutile, anatase, and brookite, respectively.

**Activity Measurements.** Catalytic CO oxidation activity data for different titania-supported catalysts were obtained and the results are described in more detail elsewhere.[12] Typically, 50 mg Au−$TiO_2$ catalyst was packed into a 4-mm-ID quartz U-tube, supported by quartz wool. Sample treatments were carried out on the same instrument. During reactions, a gas stream of 1% CO balanced with dry air (<4 ppm water) was flowed at ambient pressure through the catalyst at a rate that was adjusted to maintain a constant space velocity of 40 000 mL/(h $g_{catalyst}$). Gas exiting the reactor was analyzed by a Buck Scientific 910 gas chromatograph equipped with a dual molecular sieve/porous polymer column (Alltech CTR1) and using a thermal conductivity detector. The data are shown as lightoff curves, displaying conversion vs temperature.

**X-ray Absorption Spectroscopy (XAS).** The XAS data at the Au $L_{III}$-edge were collected at beamline X18b at the NSLS, Brookhaven National Laboratory. The storage ring operated at 2.5 GeV with a current between 200 and 300 mA. A Si (111) crystal was used as a monochromator and the crystal was detuned by 20% at the Au $L_{III}$-edge to reject higher harmonics. The X-ray absorption was measured in transmission mode using an ion chamber placed in the beam path, and in fluorescence mode using a large-area Passivated Implanted Planar Silicon (PIPS) detector perpendicular to the upcoming beam. To avoid thickness effects, the samples were prepared with a thickness to satisfy the condition that the absorption edge step, $\Delta\mu x$, be less than 1 at the Au $L_{III}$-edge. The samples were also assumed to be highly uniform, since, as shown below, the Au particle size was less than 10 nm.

The spectroscopic measurements were performed using two distinct experimental setups. In one setup, the catalysts were pretreated in a quartz reactor tube, in which the temperature and the flowing gases were controlled and selected for a given pretreatment condition. Following the pretreatment, the catalysts were transferred through ambient air to a cryogenic sample holder where the XAS experiments were performed.

In another setup, which was only available to us when performing the studies of the Au catalysts supported on the different allotropic forms of $TiO_2$, the catalysts were treated in situ in a quartz reactor with Kapton windows for transmission and fluorescence measurements so that the catalysts were never exposed to ambient air. The reactor allowed experiments at high temperatures and at liquid nitrogen temperatures.[15] Therefore, XANES spectra could be obtained during pretreatment at higher temperatures, whereas EXAFS could be performed under He after cooling the reactor cell to liquid $N_2$ temperatures to minimize the thermal disorders that can lead to high Debye−Waller factors. As will be reported, the results obtained with the in situ reactor indicate that the oxidation state of Au is not altered when the catalyst is exposed to air. Therefore, the first ex situ setup used should not have altered the Au oxidation state.

The gases employed during treatment were He (Matheson, 99.995%), 4% $H_2$/He (Matheson, $H_2$ 99.99% + He 99.995%), 1% CO/air (Air Liquid, <4 ppm water), and dry air (Matheson, zero gas). During the EXAFS measurements, He was passed through a water/oxygen removing purifier.

The program XDAP (version 3.2) was used to analyze and fit the data.[16] The data reduction procedure consisted of the following steps: spectra averaging, preedge subtraction, background determination, and normalization. First, the preedge was approximated by a modified Victoreen curve and subtracted from the whole data range. The edge position is defined to be the first inflection point on the leading absorption peak. This was calibrated to be 11 919 eV for the $L_{III}$-edge of a Au reference foil. The background in the EXAFS region was approximated using a cubic spline routine and optimized according to the criteria described by Cook and Sayers.[17] Then, the spectra were normalized by the edge-step at 50 eV after the absorption edge. The $k^3$-weighted and $k^1$-weighted EXAFS functions were Fourier transformed, filtered, and fitted in $R$ space. Considering the fact that an EXAFS spectrum can be composed of several shells, the aims of filtering are to isolate the contributions of specific shells and to eliminate low-frequency background and high-frequency noise. Fourier filtering is done by choosing a window in the Fourier transform spectrum and calculating the inverse Fourier transform of the selected $R$-range. The interatomic distance ($R$), the coordination number (CN), the difference of the Debye−Waller factor from the reference ($\Delta\sigma^2$), and the correction of the threshold energy ($\Delta E°$) were treated as free parameters during the fitting. The number of free parameters is, however, limited by the $k$-range used and by the $R$-range of the fitted window, according to the Nyquist theorem.[18] The quality of the fit was estimated from the values of $k^3$ variance ($V_{k^3}$). The variance represents the residual between the observed and calculated spectrum in the fitted range. Low values of variance indicate a good agreement between data and model. Fitting analysis in both $k^1$- and $k^3$-weighted Fourier transforms was applied to obtain a unique set of CN and $\Delta\sigma^2$ parameters. Those parameters are highly correlated and there are a number of different combinations of CN and $\Delta\sigma^2$ that can lead to similar fits. However, the set of combinations depends on the $k$ weight factor. Therefore, a unique set of parameters might be found by fitting on both $k^1$- and $k^3$-weighted Fourier transforms. To analyze the spectra, simulations of reference compounds using FEFF8.1[19] were used to calculate phase shifts and backscattering amplitude. FEFF references were obtained for Au−Au and Au−O using crystallographic data of Au metal and $H_2Pt(OH)_6$, respectively, since the phase shift and backscattering amplitude of Au and Pt hardly differ.[20] For the fitting analysis, fluorescence spectra were used when the sample was very diluted. Consequently, the jump was

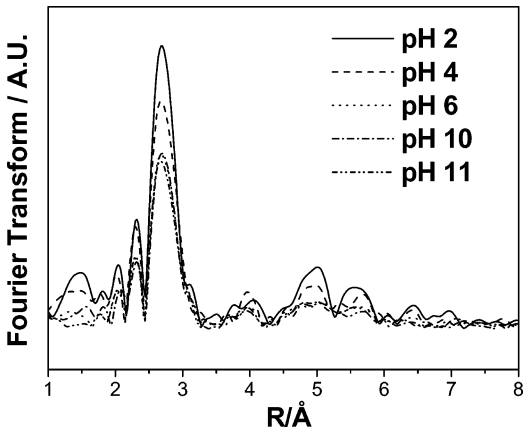


**Figure 1.** Magnitude of the Au $L_{III}$-edge $k^3$-weighted Fourier transform of Au on P-25 prepared using precursor solution of variable pH.

very small. However, in many cases both spectra were fitted to verify the results.

The edge jump and the XANES portions of the spectra provided quantitative information on the concentration of Au metal present in the supported catalyst and information regarding changes on the Au oxidation state, respectively. The total amount of Au element present on the sample was estimated by measuring the height of the absorption step edge in the EXAFS spectrum measured by transmission. The absorption step height is directly proportional to the areal density, g $cm^{-2}$. The samples were pressed into a sample holder of known area and the amount of Au could then be determined by comparing the step height to that obtained from a 10-$\mu$m Au foil. Changes in the oxidation state of the Au catalysts were obtained by comparing the first absorption peak intensities with the reference materials, Au foil and $Au_2O_3$, after the data were normalized by the edge jump.

## Results

**Au on Nanocrystalline $TiO_2$ Prepared from Solutions with Variable pH.** These samples consisted of Au supported on $TiO_2$ (P-25) prepared by D−P at various pH. Figure 1 shows the absolute parts of the Fourier-transform $\chi(k)\cdot k^3$ Au $L_{III}$-edge of the samples that were pretreated ex situ in air at 400 °C for 2 h. The spectra obtained at −183 °C contain peaks that correspond to Au−Au shells in a Au metal cluster of face-centered cubic (fcc) lattice.

The size of the Au particles can be estimated by Au cluster models with varying numbers of atoms and by calculating the average coordination number. For particles smaller than 5 nm, the coordination number is a strong and nonlinear function of the particle diameter, and the accuracy of this method is higher for smaller metal clusters since the average coordination number for bigger particles approaches the expected bulk value. Assuming a typical error of 10% in a first-shell coordination number obtained by the EXAFS analysis, this method is only feasible and widely used in EXAFS to determine the size of particles smaller than 5 nm.[21,22,23] For instance, Frenkel[21] calculated average coordination numbers from the first to the fifth shell for a Pt fcc structure as a function of the number of atoms, assuming different models of nanoparticles, such as cuboctahedron and hemispherical cuboctahedron with different basal plans. It is important to note that the particle size is dependent on the particle geometry assumed. The correlation between the first-shell coordination number and the particle size for a hemispherical cuboctahedron cluster model determined by Frenkel was used to obtain the particle size in Figure 2.[21]

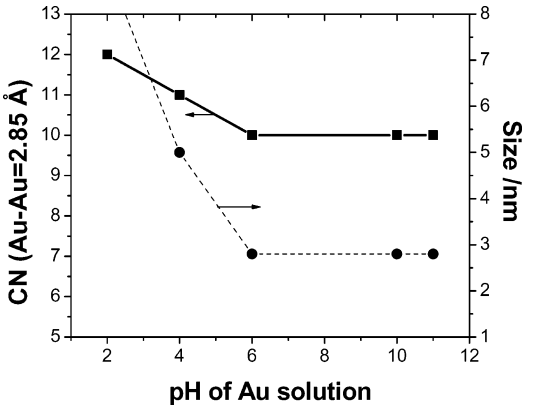


**Figure 2.** Relationship between coordination number, particle size, and pH of Au precursor solution.

**TABLE 1: Results of the $k^3$-Weighted Curve Fitting of the Au $L_{III}$-edge of the Au Catalysts Supported on P-25 Prepared Using Precursor Solution of Variable pH**

| sample | shell | CN | $R$, Å | $\Delta\sigma^2/10^{-4}$ Å$^2$ | $\Delta E°$/eV | $V_{k^3-fit}$ |
|---|---|---|---|---|---|---|
| pH = 4 | Au−O | 2.9 | 1.98 | −13 | 0.1 | 1.9 |
| | Au−Cl | 0.9 | 2.28 | −25 | −17 | |
| pH = 6 | Au−O | 2.7 | 1.98 | −29 | −0.4 | 0.4 |
| | Au-Cl | 0.7 | 2.24 | 19 | −14 | |
| pH = 10 | Au−O | 3.2 | 1.98 | −30 | −2.1 | 0.4 |

[a] The errors in the final parameters are expected to be CN ± 10%, $R$ ± 0.02 Å, $\Delta\sigma^2$ ± 20%, and $\Delta E°$ ± 20%. [b] The $k$ and $R$ ranges used for the fittings were $\Delta k$ = 3.2/16.3 Å$^{-1}$ and $\Delta R$ = 4 Å. [c] Analysis based on the fluorescence data.

The coordination numbers were obtained by fitting the first shell of the EXAFS spectra of Figure 1.

For the sample prepared using pH = 2, the first-shell coordination number is 12, which is the same as for a bulk Au cluster. In this case, the size cannot be estimated by using EXAFS. It is very important to stress that EXAFS analysis of particle size is accurate only if the metal particles are small and the particle size distribution is narrow. For samples prepared using pH > 6, the particles are estimated to have an average size of 2.8 nm (Figure 2). The trend obtained corroborates previous results in the literature,[1,24] where particle sizes were estimated by transmission electron microscopy (TEM). Haruta[1] reported Au particles on $TiO_2$ smaller than 4 nm when the precursor solution had a pH > 6. Zanella et al.[24] used high Au loadings (as high as 8% of Au in $TiO_2$) and obtained particles smaller than 2.0 nm for pH > 6.

Analysis of the samples prior to pretreatment in air revealed two distinct cases (Table 1): at lower pHs the presence of oxygen and chlorine neighbors, and at higher pHs the presence of only oxygen neighbors. These results are as expected from the speciation of the Au precursor in aqueous solution. As pH increases, an increasing amount of $Cl^-$ is displaced from the $Au(Cl)_4^-$ and is replaced by $OH^-$, both in the solution and adsorbate species.[25] At pH > 8 most Au precursor is converted to $Au(OH)_4^-$.

The Au loadings determined by the edge jump values were 1.0, 2.0, 3.9, 4.7, and 2.7% for pH of 2, 4, 6, 10, and 11, respectively.

**Au on Mesoporous $TiO_2$ with Variable Loading.** For the purpose of investigating changes in the metal oxidation state and particle size with variable Au loading, we used a mesoporous titania support. The mesoporous titania support was developed with mean pore diameters in the range of interest for Au catalysts as an attempt to control the Au particle size.

As already described, the total amount of Au element present

**TABLE 2: Results of the $k^3$-Weighted Curve Fitting of the Au $L_{III}$-edge of the Au Catalysts Supported on Mesoporous Titania**

| synthesis loading (experimental)[b] | conditions | shell | CN | $R$, Å | $\Delta\sigma^2$/ $10^{-4}$ Å$^2$ | $\Delta E°$/ eV | $V_{k^3-\mathrm{fit}}$[c] |
|---|---|---|---|---|---|---|---|
| 2.5% | 4% $H_2$, RT | Au−O | 1.5 | 1.97 | −2.1 | 4.7 | 1.5 |
| (2.8%) | | Au−Au | 6.0 | 2.86 | 2.7 | −2.5 | |
| | 4% $H_2$, 100°C | Au−Au | 11 | 2.86 | 0.1 | −2.9 | 0.9 |
| | 4% $H_2$, 200°C | Au−Au | 11 | 2.87 | −6.8 | −4.2 | 1.0 |
| 5% | 4% $H_2$, RT | Au−Au | 7.5 | 2.86 | 15 | −4.7 | 0.8 |
| (4.7%) | 4% $H_2$, 100°C | Au−Au | 8.0 | 2.86 | 18 | −4.6 | 1.7 |
| | 4% $H_2$, 200°C | Au−Au | 7.3 | 2.86 | 11 | −5.5 | 1.6 |
| 10% | 4% $H_2$ | Au−Au | 11 | 2.85 | 13 | −1.4 | 7.0 |
| (7.1%) | 4% $H_2$, 100°C | Au−Au | 11 | 2.85 | 13 | −1.6 | 5.7 |
| | 4% $H_2$, 200°C | Au−Au | 9.5 | 2.86 | 11 | −3.7 | 0.7 |

[a] Errors in the final parameters are expected to be CN ± 10%, $R$ ± 0.02 Å, $\Delta\sigma^2$ ± 20%, and $\Delta E°$ ± 20%. [b] Au loading estimated by the edge-jump measurements. [c] Percentage difference between the $k^3$-weighted experimental data and the model. [d] $k$ and $R$ ranges used for the fittings were $\Delta k = 3.4/16$ (for the 2.5% and 10% loading samples), $\Delta k = 3.4/17.4$ Å$^{-1}$ (for the 5% loading samples), and $\Delta R = 4$ Å. [e] Analysis of the 2.5% loading samples based on the fluorescence data, whereas the fittings of the 5% and 10% were based on the transmission data.

was determined by the height of the edge jump. The edge jump was measured for the three samples prepared on mesoporous titania with synthesis Au loadings of 2.5, 5, and 10 wt %. By comparing the synthesis Au loading with the measured values (Table 2), it can be observed that, at low loadings, the titania retains most of the Au from the impregnated solution. At higher loadings, the retention decreases.

The intensity of the white line, which is the first absorption peak centered 4 eV above the edge (around 11 923 eV for the Au $L_3$-edge), in a XANES spectrum is related to the density of unoccupied d states.[26] Therefore, any variations of the density of unoccupied states due to changes in the oxidation state will be reflected in the intensity of the white line. Our goal is to derive conclusions regarding the presence of cationic and/or reduced Au after variable pretreatment protocols and under reaction conditions by comparing the white-line intensity obtained for each catalyst with the ones obtained from the reference compounds Au foil ($Au^0$) and $Au_2O_3$ ($Au^{3+}$). It is possible that Au, in the reference compound $Au_2O_3$, is actually present in a more reduced state than $Au^{3+}$. This is because, in general, $Au_2O_3$ can be reduced once exposed to light. Therefore, the degree of Au oxidation should be considered a lower limit. Figure 3 depicts the XANES spectra of the two reference materials and the Au on mesoporous titania with variable loadings. For each catalyst, a spectrum was recorded for the fresh catalyst, after treatment with 4% $H_2$/He at room temperature for 1 h, after treatment with 4% $H_2$/He at 100 °C for 1 h, and after treatment with 4% $H_2$/He at 200 °C for 1 h (Figures 3a, 3b, and 3c). The XANES spectra of the samples after treatment at 200 °C were identical to the ones treated at 100 °C. Therefore, we omitted the former case from the figures. It should be noted that, in all cases, we used the experimental setup where the catalysts were treated in a quartz reactor cell and transferred to the cryogenic sample holder after they were exposed to atmosphere.

The fresh catalysts revealed the presence of cationic Au with an average oxidation state slightly inferior to the one presented by Au in the $Au_2O_3$ compound, as indicated by the relatively smaller white line of the fresh catalyst compared to that of $Au_2O_3$. It is probable that a mixture of hydroxide and reduced Au was present, with $Au^{3+}$ predominant. For all samples, after treatment in $H_2$ at 100 °C, the white line is essentially absent

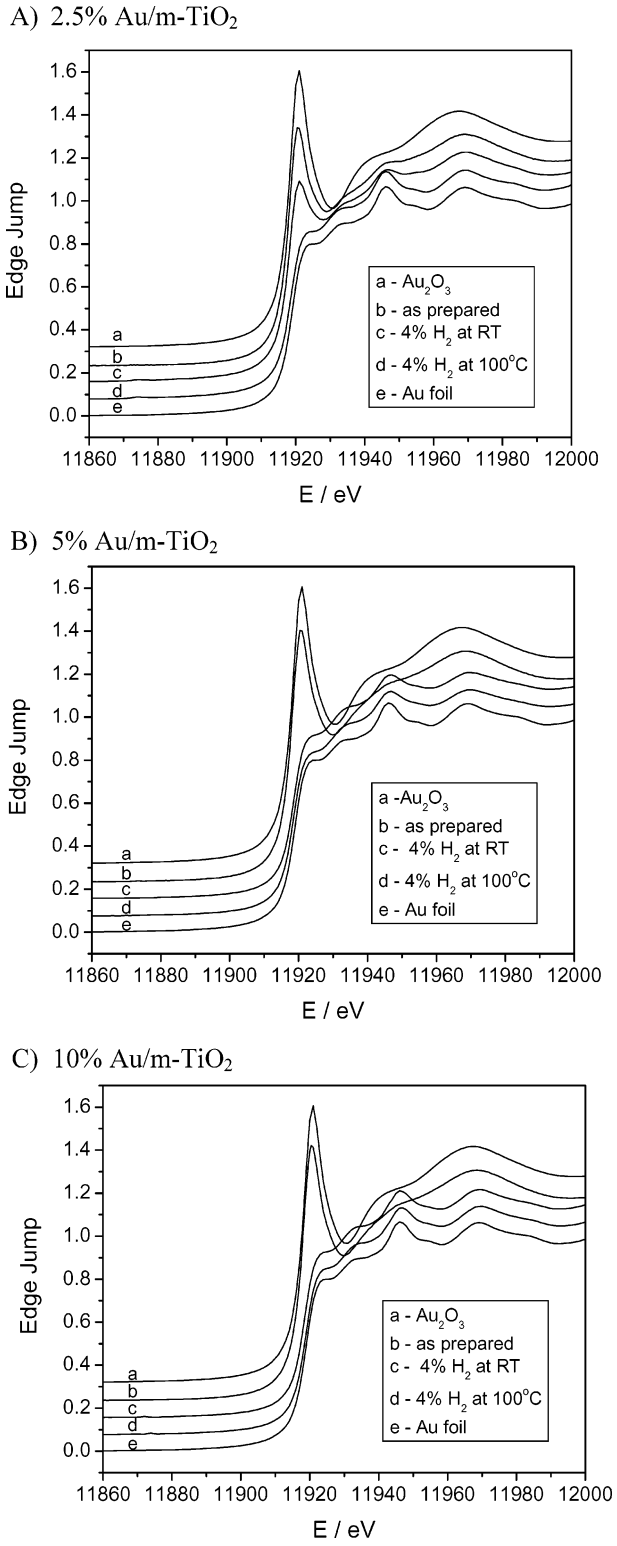


**Figure 3.** XANES of the (A) 2.5% Au/m-$TiO_2$, (B) 5% Au/m-$TiO_2$, and (C) 10% Au/m-$TiO_2$ after different pretreatment conditions. The curves were offset vertically.

and the spectrum is similar to that of Au foil, indicating that no observable cationic Au remains. In some cases (e.g., in Figure 3b), the oscillations at energies above 11 920 eV are not quite as pronounced for the reduced catalysts as for Au foil, an effect attributable to the smaller Au particle size in the reduced sample compared to bulk Au. In close examination of the spectrum from the Au foil, a small peak is found to be present at the position of the white line for the Au foil, which is actually

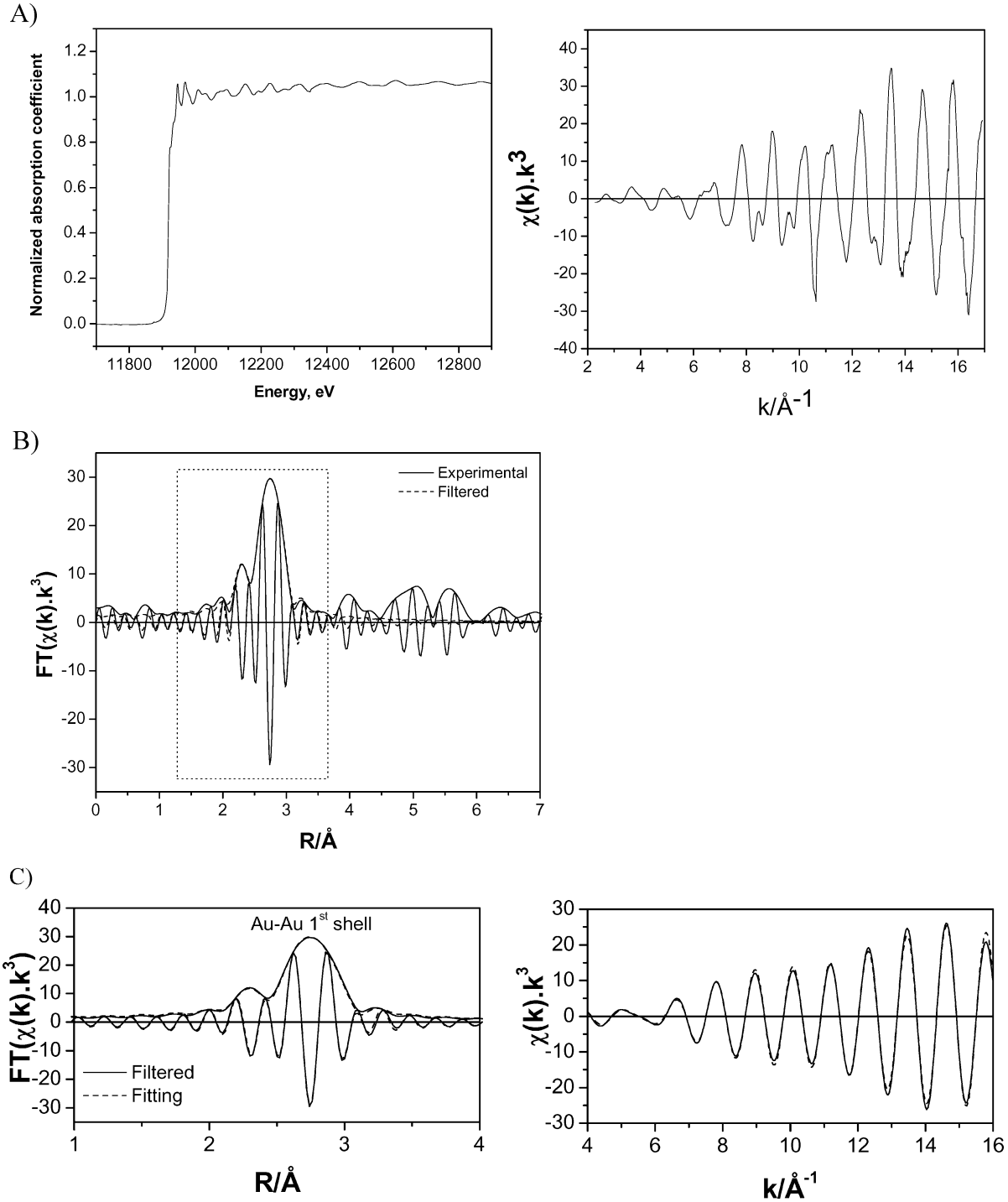


**Figure 4.** EXAFS data of 5% Au/m-$TiO_2$ after treatment with 4% $H_2$/He at 200 °C: (A) X-ray absorption spectra after preedge subtraction and normalization, and $k^3$-weighted $\chi(k)$; (B) Fourier-transformed $k^3$-weighted EXAFS function and filtered data (The dashed rectangle represents the window isolating the first Au−Au shell); (C) Comparison between the filtered and the fitting EXAFS curves.

slightly more pronounced than for the Au catalysts reduced at 100 °C. The differences can be attributed to several factors that can also affect the density of d-electrons other than changes in oxidation number, such as the particle sizes and the interactions with the support.[27]

Although the sample with lower loading (Figure 3a) presents the lower initial oxidation state (lower white line intensity), it is the most difficult to achieve a completely reduced state. The samples with synthesis loading of 5 and 10% are already completely reduced after flowing 4% $H_2$ at room temperature (Figures 3b and 3c), whereas the 2.5% Au sample is only completely reduced after heating to 100 °C in 4% $H_2$.

The results for the EXAFS analysis are given in Table 2 for fittings in *R* space and $k^3$-weighted Fourier transforms. Similar results were obtained when fitting the $k^1$-weighted Fourier transforms. The average EXAFS absorption spectra of the four data sets measured after reduction at 200 °C of 2.5% Au/m-$TiO_2$ are presented in Figure 4a. In this figure, the raw data after preedge subtraction and normalization are presented together with the EXAFS spectrum as a function of the wave vector, *k*. Figure 4b shows the next steps during the data reduction of the raw data, namely the production of the Fourier transform function and of the filtered spectrum. A comparison between the filtered data and the first shell fit is given in Figure

4c. This data reduction and analysis process is representative of a fitting of the first Au−Au contribution. Note that, because of the phase shifts, the distances observed in the Fourier-transformed spectra are always shorter than the real absorber−backscatterer distances (Table 2).

As already observed in the XANES spectra (Figure 3a), the catalyst with the lowest loading was still slightly oxidized after treatment with 4% $H_2$ at RT, which is revealed by the presence of a Au−O contribution at 1.95 Å. However, after reduction at higher temperatures (200 °C), this sample presented the highest Au−Au coordination numbers when compared to the others containing higher Au loadings. The higher coordination numbers should be indicative of bigger particles that are being formed on the mesoporous titania surface. The low Debye−Waller factors obtained in this case as well indicate that the particles have a lower degree of static disorder, since the temperature of EXAFS measurements was kept constant for every sample. The static disorder is an intrinsic structural property of the system, whereas thermal disorders can be reduced by lowering the temperature. The catalyst with intermediate Au loading presents the lowest coordination number, whereas the catalyst with the highest loading presents an intermediate Au−Au coordination number after treatment at 200 °C. Although the coordination number in the 10% Au synthesis loading case seems to be higher after treatment at RT and 100 °C than at 200 °C, these two fittings are of very poor quality when compared to all the others. The quality of the fit can be evaluated by the $k^3$-variance (Table 2), which gives the percentage difference between the $k^3$-weighted experimental data and the model. The high variances obtained for the fittings of the 10% Au after treatment at RT and 100 °C reveal the above-mentioned poor quality of these two fittings. Therefore, the coordination numbers obtained in these cases should have a higher uncertainty, whereas the values for the fitting after treatment at 200 °C are more reliable.

**Au on Different Allotropic Forms of Nanocrystalline $TiO_2$.** The next catalysts studied comprised the group of Au supported on nanocrystalline titania. The supports used were the commercial P-25 (contains 70 wt % anatase and 30 wt % rutile), as well as pure forms of anatase, rutile, and brookite. To carefully study the oxidation state of Au under controlled atmospheres and temperatures, as well as under reaction conditions, all of the following XAS measurements were performed using the in situ quartz reactor. Therefore, the XANES measurements were taken at the temperature indicated and without exposing the catalysts to ambient atmosphere. The same is true for the EXAFS data, with the difference that, during the measurements, the samples were brought to liquid $N_2$ temperature in flowing He.

The first set of experiments consisted of measuring the XANES portion of the absorption spectra of the catalysts as inserted, followed by flowing 1% CO in air at RT to mimic the gases present during the CO oxidation reaction (Figure 5a). Several measurements were taken during the interval of 1 h while flowing the gas mixture containing CO and $O_2$. Then, a XANES spectrum was taken for each sample after the sample was heated to 150 °C under He for 30 min. Finally, another measurement was taken after switching the gas to a reducing atmosphere of 4% $H_2$/He at 150 °C for 30 min. The XANES results presented in Figure 5 were obtained for the Au on an anatase support and illustrate well the transformations that occurred on all the allotropic forms of the titania-supported catalysts. We can first observe a continuous reduction of the Au cations under 1% CO/air, even at room temperature. The catalyst is further autoreduced in He at 150 °C, but complete

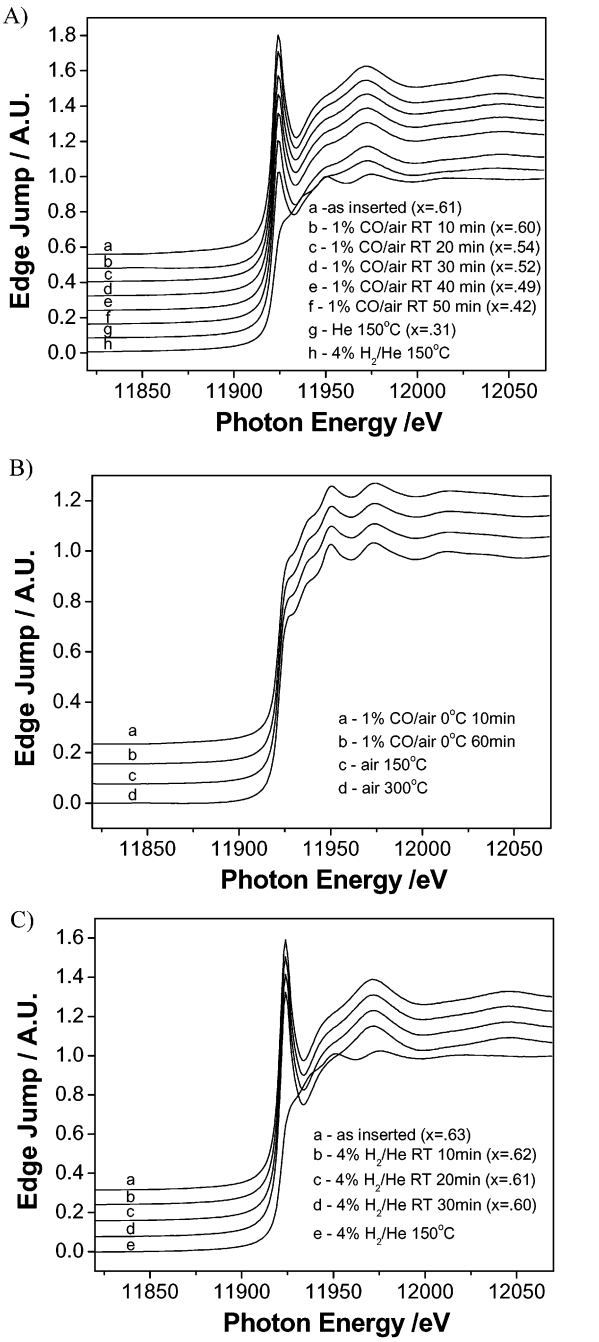


**Figure 5.** XANES of the Au/anatase after different pretreatment protocols. The curves were offset vertically. In Figures 5a and 5c, the value 'x' indicates the difference between the peak height of each normalized spectrum and the sample after treatment in 4% $H_2$/He at 150 °C.

reduction to $Au^0$ is achieved under 4% $H_2$ at 150 °C. The continuous reduction is even more evidenced by subtracting each normalized spectrum from the sample after treatment under 4% $H_2$ at 150 °C and recording the peak height difference (value x in Figures 5a and 5c).

After complete reduction was obtained in $H_2$ at 150 °C, the reactor was cooled to 0 °C, and the gas was switched again to 1% CO/air to observe if reoxidation of the catalysts could occur at low temperatures typical for the CO oxidation reaction (Figure 5b). The Au catalysts, however, remained at a reduced state under these conditions, and remained so even after flowing air at higher temperatures (150 and 300 °C).

**TABLE 3: Results of the $k^3$-Weighted Curve Fitting of the Au $L_{III}$-edge of the Au Catalysts Supported on Allotropic Titania**

| catalyst | conditions | shell | CN | $R$, Å | $\Delta\sigma^2$/ $10^{-4}$ Å$^2$ | $\Delta E°$/ eV | $V_{k^3-\text{fit}}$ |
|---|---|---|---|---|---|---|---|
| Au/P-25 | 4% $H_2$/He 150°C | Au−Au | 6.7 | 2.80 | 39 | −6.6 | 1.02 |
| | air 300°C | Au−Au | 9.7 | 2.83 | 32 | −8.2 | 1.74 |
| Au/anatase | 4% $H_2$/He 150°C | Au−Au | 7.7 | 2.83 | 41 | −9.5 | 1.29 |
| | air 300°C | Au−Au | 9.0 | 2.84 | 28 | −9.4 | 0.72 |
| Au/rutile | 4% $H_2$/He 150°C | Au−Au | 8.3 | 2.82 | 39 | −8.9 | 0.65 |
| | air 300°C | Au−Au | 10.2 | 2.86 | 16 | −9.8 | 0.28 |
| Au/brookite | 4% $H_2$/He 150°C | Au−Au | 0.45 | 2.72 | −29 | −20 | 1.45 |
| | | Au−Au | 7.5 | 2.82 | 32 | −8.3 | |
| | air 300°C | Au−Au | 7.0 | 2.85 | 27 | −10 | 2.12 |

[a] Errors in the final parameters are expected to be CN ± 10%, $R$ ± 0.02 Å, $\Delta\sigma^2$ ± 20%, and $\Delta E°$ ± 20%. [b] Minimum $k$ and $R$ ranges used for the fittings were $\Delta k = 3.6/16$ Å$^{-1}$and $\Delta R = 4$ Å. [c] Analyses of the Au on P-25, anatase, and rutile were based on the transmission data, whereas analysis of Au on brookite was based on fluorescence data.

In another set of experiments, a fresh catalyst was inserted into the reactor and XANES measurements were performed with a constant flow of 4% $H_2$/He at room temperature during an interval of 30 min (Figure 5c). Negligible reduction was observed at RT in this case. Again, Au was only completely reduced after raising the temperature to 150 °C.

The EXAFS-fitting results at liquid nitrogen temperature are presented in Table 3 for the following two cases: after pretreatment in 4% $H_2$/He at 150 °C and after subsequent treatment in air at 300 °C. It can be observed that the coordination numbers for the Au−Au shells increase after air treatment at 300 °C, which is an indication of particle aggregation. Additionally, the first shell shifts to longer distances after treatment at 300 °C, approaching the bulk atomic distance of 2.88 Å. In the case of Au on brookite, the fit was more complicated for the sample reduced at 150 °C. This was because the peak corresponding to the closest atomic shell was broadened and a single-shell model resulted in a poor fit. Table 3 shows an attempt to account for the broadening by using two Au−Au shells. This resulted in a better fit but it yielded large negative numbers for the $\Delta\sigma^2$ and $\Delta E°$ parameters, indicating that a more complex shell distribution and analysis would likely be the case. Despite the problems of the fitting, both attempted models resulted in a clear shortening of the Au−Au bond after treatment at 150 °C, as well as a small variation between the coordination numbers after treatment at 150 °C and subsequent treatment at 300 °C. Therefore, there is no indication of particle aggregation after higher temperature treatments for Au on brookite.

It is of interest to correlate the catalytic activity of the Au samples with the oxidation state measured by XANES and with the particle sizes as measured by EXAFS. Representative measurements are shown in Figure 6 for the Au/$TiO_2$ (rutile) sample.[12] Data in Figure 6 show the lightoff curves for a single sample after exposing to a sequence of pretreatment steps. The pretreatment steps consisted (in this specific order) of heating in Ar at 150 °C for 30 min, exposing to 12% $H_2$−Ar at 150 °C for 30 min, exposing to 8% $O_2$−He at 150 °C for 30 min, and exposing to 8% $O_2$−He at 300 °C for 30 min. Between each pretreatment, the sample was cooled rapidly to room temperature in the treatment mixture, the gas was switched to the reactant mixture, and then a lightoff curve was measured from lowest to highest temperature.

It is seen in Figure 6 that, following treatment at 150 °C in Ar, the sample is active for CO oxidation. However, the activity is improved by treatment at 150 °C in $H_2$. Following the $H_2$ treatment, the sample exhibits 50% conversion at −35 °C. From

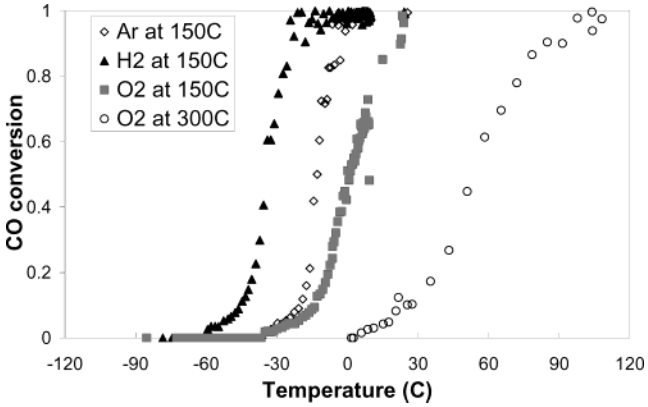


**Figure 6.** Lightoff curves showing the CO conversion as a function of temperature for Au on a rutile sample following four different treatments.

the reactor flow and the Au weight loading, the specific rate at −35 °C is $2 \times 10^{-3}$ $\text{moles}_{CO}/(\text{moles}_{Au}\ s)$, which is comparable to that observed for other active Au catalysts supported on $TiO_2$. As described above, the XANES data imply that treatment in inert atmosphere (Ar or He) at 150 °C may not completely reduce the Au, but treatment in $H_2$ at this temperature is effective in completely reducing the Au in all of the Au/$TiO_2$ samples (Figure 5a). Therefore, the high activity state corresponds to Au in a fully reduced state. The precursor oxidized state exhibits activity because the reaction gas itself (1% CO in air) also reduces some of the Au in the catalyst bed, as demonstrated by the XANES. We propose that it is this reduced portion that carries out the CO conversion.

Subsequent treatments in oxygen of the Au/$TiO_2$ (rutile) bring about a decrease in activity, as indicated by the increased lightoff temperatures seen in Figure 6. This decrease in activity cannot be associated with an oxidation of the Au, since XANES indicates that the Au remains in a fully reduced state. The variation in activity following these pretreatments presented for Au on rutile was also exhibited by Au on the anatase, as well as brookite supports that were pretreated in exactly the same protocol. In each case, the most reactive state was after the treatment in $H_2$, although for the anatase the Ar-treated sample was almost as active. Treatment at higher temperature brought about a decrease in activity, although the decrease was only slight in the case of brookite.

It is assumed that the loss of activity observed following the oxygen treatments at 300 °C is associated with growth of particle size due to sintering. The occurrence of the sintering is dependent upon the type of $TiO_2$ support. Of the three titania allotropes, the activity of the Au supported on rutile was the most sensitive to treatment at 300 °C in oxygen; the activity of the Au supported on brookite was the least sensitive.[12] This order of sensitivity matches the changes in Au particle sizes as demonstrated by the EXAFS, where rutile exhibits a significant increase in Au first-shell coordination number upon treating in air at 300 °C, while brookite exhibits little change (Table 3).

A comparison of the activity for CO oxidation and the mean Au particle size determined by EXAFS is provided in Figure 7. The activity is described as the $T_{50}$, the temperature at which the conversion reaches 50%. This is a nonlinear indication of reaction rate, but it is used since it permits comparison of activity for samples that have rates that vary by too much to be measured at a single temperature. The particle size is estimated using the hemispherical cuboctahedron model,[21] given the Au−Au first shell coordination number, which is obtained directly from the EXAFS. By these measures, it is seen that there is a correlation

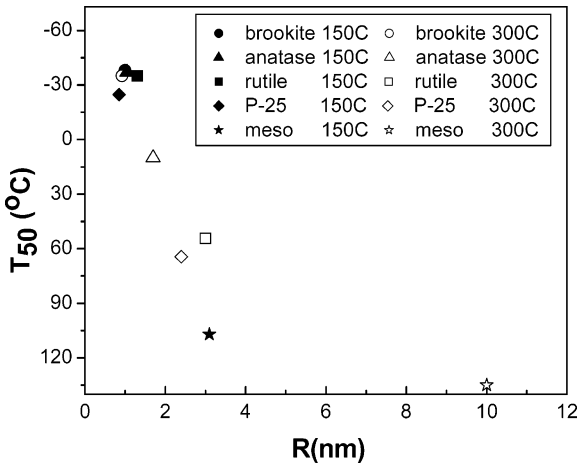


**Figure 7.** Relationship between activity on CO oxidation and particle size.

between the Au particle size and the activity. Data are given for each sample following the treatment in $H_2$ at 150 °C and following the treatment in $O_2$ at 300 °C. It should be noted that, in the case of Au supported on m-$TiO_2$ and treated at 300 °C, the particle size is already above the accuracy of an EXAFS measurement, since the average coordination number for bigger particles approaches the expected bulk value. Therefore, the 10-nm size should be seen only as a lower limit. These samples all had comparable Au loadings. Since particle growth causes surface area loss, the decrease in activity might be explained by Au surface area loss. Again, since the lightoff temperature is not a linear measure of activity, it is not possible to determine from these data if the activity falls faster than expected from the decrease in dispersion, which would indicate a size effect rather than a dispersion effect.

## Discussion

The EXAFS enables the identification of several factors that can control the particle size and ultimately the activity of gold catalysts, such as the pH of the precursor solution, the Au loading, the pretreatment conditions, and the support structure. For instance, EXAFS results obtained for the set of samples prepared using precursor solutions with different pH on $TiO_2$ (P-25) confirm the applicability of this type of analysis. It is clear that the technique can probe sizes of interest for the catalysis of gold, while it cannot be applied when the particle size is bigger than a certain threshold (~5 nm), where other techniques, such as TEM, are more suitable. As observed in Figure 2, the expected trend reported first by Haruta[1] was reproduced and particles smaller than 4 nm were obtained and detected by EXAFS when the pH was adjusted to be higher than 6.

The effect of Au loading on the particle size and reducibility of Au clusters was studied using the mesoporous titania as support. The most striking observation was that, for lower Au loadings, a higher Au−Au coordination number was obtained after treatment with 4% $H_2$/He at 200 °C (Table 2). The higher coordination number is an indication of larger metallic particles. The reasons are still unclear why the catalyst containing the least amount of Au would also present the bigger particles, but similar results were obtained using transmission electron microscopy (TEM) analysis (data not shown). If we are to believe that the larger particles reside on the external surfaces while the smaller ones are confined within the mesopores, then most of the particles on the 2.5% Au/m-$TiO_2$ would be present at the external surface. On the other hand, EXAFS is a technique that gives an average value for the particle size. Therefore, the existence of big particles on the external surface might increase the average coordination number, even if very small particles coexist inside the pores. Additionally, the catalyst with the low Au loading had the lower reducibility (Figure 3), which could be due to the fact that bigger Au aggregates are less easily reduced.

The XANES study during pretreatment and reaction conditions (Figures 3 and 5) provide insight into the oxidation state and the transformation undergone by Au atoms on the titania support. Variation of the titania crystalline structure does not seem to affect the redox behavior of the Au clusters, since no substantial difference appeared when testing the XANES of Au supported on P-25, rutile, anatase, or brookite. For all the samples analyzed, the Au precursor was completely reduced to $Au^0$ after treatment in 4% $H_2$/He at 150 °C. The Au on mesoporous titania at the three different loadings also exhibited similar redox behavior, except for the slightly more sluggish reduction of the 2.5% Au sample at room temperature. All samples were most active after reduction at 150 °C, implying that the fully reduced state is the most active. Furthermore, once the Au atoms were reduced, no reoxidation occurred, even after treatment in air at 150 °C or 300 °C. It is also very important to observe the behavior of Au under a mixture of CO and air, to mimic the reaction conditions. A gradual reduction of the Au precursor was clearly observed when 1% CO/air was present at room temperature (Figure 5a), even though the concentration of oxygen is 20 times higher than that of the reductant. Once fully reduced in $H_2$, the introduction of the reaction mixture did not bring about oxidation of the Au observable by XANES (Figure 5b). These observations imply that reaction conditions also drive the sample irreversibly toward the fully reduced state.

Although the Au precursor is reduced by the reaction mixture, and presumably by CO itself, almost no change of oxidation state was detected in the case of flowing 4% $H_2$/He at room temperature (Figure 5c). This phenomenon may be responsible for the high activity of small Au particles for the preferential oxidation of CO in the presence of excess hydrogen (PROX) reaction.[28]

The following can be derived from our XANES results in conjunction with the reactivity tests: (1) Au is present as $Au^0$ after treatment in $H_2$ at 150 °C, (2) Au is still reduced under reaction conditions and no reoxidation occurs, (3) Au is highly active for CO oxidation after treatment in $H_2$ at 150 °C conditions that lead to $Au^0$. This last observation does not corroborate the Bond−Thompson model,[4] in which the active phase would be composed of both gold atoms and ions. Previous work on Au supported on $Fe_2O_3$,[8] $CeO_2$,[10] MgO,[9] and $Al_2O_3$[28] seems to support the Bond−Thompson model. However, there are also persuasive arguments and data that do not support this model.[29] Most recently, Guzman and Gates,[5,6,9] using XANES, found both $Au^+$ and $Au^0$ (but no $Au^{3+}$) present under reaction conditions in a ratio that depends on the CO partial pressure. Under steady-state reaction conditions of 1.4% CO and 20% $O_2$ at 373 K, they found optimal activity while oxidized Au exceeded reduced Au with a $Au^+$:$Au^0$ ratio of 3:2. By comparing Mössbauer spectroscopy with activity on three catalysts of Au supported on iron oxide, Hodge et al.[8] found that their most-active catalysts had a $Au^{3+}$:$Au^0$ ratio of 3:2. These catalysts exhibited characteristic Mössbauer features of AuOOH in the "as-dried" state before reaction, but they were not tested after exposure to the reaction mixture. Samples calcined to 400 °C had substantially lower activity and showed exclusively $Au^0$

(and also larger Au particles). Hodge et al.'s and our results are similar, showing that the "as-dried" samples contained $Au^{3+}$ cations while those calcined to 300 °C were entirely Au neutral, had larger particles, and had lower activity.

Finally, it has been proposed that deactivation observed in Au on $Al_2O_3$ catalysts can be explained by loss of cationic Au necessary for stabilizing hydroxyls present during high activity.[30,31] However, to date there appears to be no published direct spectroscopic evidence of cationic Au present on $Al_2O_3$ under reaction conditions. It is possible that the role of oxidized Au, or the optimal ratio of oxidized to reduced Au, for high CO oxidation activity is dependent largely on the type of support. We feel that the evidence presented here strongly supports that, in the case of titania supports, oxidized Au is not necessary for high activity.

The EXAFS results for the Au on all of the allotropic forms of titania show a common trend after treatment at 150 °C. This trend is the shortening of the Au−Au first coordination shell compared to the bond length obtained after treatment at 300 °C and bulk values, accompanied by lower coordination numbers (Table 3). The contraction of the shortest distance between two Au atoms is consistent with previous observations that show that smaller metallic particles exhibit shorter bond distances.[32] The coordination numbers increase after treatment at 300 °C under air, indicating the formation of bigger metallic particles. This is with the exception of Au supported on brookite, which did not suffer significant particle agglomeration after treatment at high temperatures. Therefore, although the catalytic activities (Figure 7) of Au supported on these different allotropic forms of titania are comparable after low-temperature treatments, the stability of the Au catalysts at higher temperatures is dependent upon the $TiO_2$ structure type.[33] Additionally, Au/brookite was the most active catalyst (lower lightoff temperatures) after calcination at 300 °C. The EXAFS-estimated coordination numbers in conjunction with the reactivity tests show a correlation between the particle size in the range studied and the activity for CO oxidation (Figure 7). However, it is not clear if the decrease in activity is due to the loss of Au surface area or to the size effect.

## Conclusion

In this study, we investigated how the oxidation state and particle size of Au clusters on nanocrystalline and mesoporous titania support varied during synthesis, pretreatment, and reaction conditions. Variation of Au loading on mesoporous $TiO_2$ shows that the lower Au loadings had the lower reducibility and the bigger Au aggregates. In situ studies of Au supported on different allotropic forms of $TiO_2$ reveal that the Au precursor is gradually reduced by flowing the reaction mixture, 1% CO/air, at room temperature and, once fully reduced, no reoxidation occurs. Comparison of lightoff curves after exposing a single sample to a sequence of pretreatment steps demonstrates that Au is in the highly active state as $Au^0$ after treatment in $H_2$ at 150 °C, indicating that oxidized Au is not necessary for high activity. In many cases, treatments at higher temperature (300 °C) brought a decrease in activity that was accompanied by an observed particle growth, and a correlation was found between particle size and activity for CO oxidation. Among the different allotropic forms of the support, Au supported on brookite did not suffer particle agglomeration and was the most active catalyst after treatment at 300 °C.

**Acknowledgment.** Research sponsored by the Division of Chemical Sciences, Geosciences, and Biosciences, Office of Basic Energy Sciences, U.S. Department of Energy, under contract DE-AC05-00OR22725 with Oak Ridge National Laboratory, managed and operated by UT-Battelle, LLC. The National Synchrotron Light Source, Brookhaven National Laboratory, is supported by the U.S. Department of Energy, Division of Materials Sciences and Division of Chemical Sciences. W. Y. and B. C. acknowledge the Oak Ridge National Laboratory Postdoctoral Research Associates Program administered jointly by the Oak Ridge Institute for Science and Education and Oak Ridge National Laboratory. The authors would like to thank Lorna Ortiz-Soto for providing the CO oxidation activity results for the Au supported on mesoporous $TiO_2$.

## References and Notes

(1) Haruta, M. *Catal. Today* **1997**, *36*, 153.
(2) Bond, G. C.; Thompson, D. T. *Catal. Rev.—Sci. Eng.* **1999**, *41*, 319.
(3) Haruta, M.; Daté, M. *Appl. Catal., A* **2001**, 222, 427.
(4) Bond, G. C.; Thompson, D. T. *Gold Bulletin* **2001**, *33* (2), 41.
(5) Guzman, J.; Gates, B. C. *J. Phys. Chem. B* **2002**, *106*, 7659.
(6) Guzman, J.; Gates, B. C. *J. Phys. Chem. B* **2003**, *107*, 2242.
(7) Davis, R. J. *Science* **2003**, *301*, 926.
(8) Hodge, N. A.; Kiely, C. J.; Whyman, R.; Siddiqui, M. R. H.; Hutchings, G. J.; Pankhurst, Q. A.; Wagner, F. E.; Rajaram, R. R.; Golunski, S. E. *Catal. Today* **2002**, *72*, 133.
(9) Guzman, J.; Gates, B. C. *J. Am. Chem. Soc.* **2004**, *126*, 2672.
(10) Fu, Q.; Saltsburg, H.; Flytzani-Stephanopoulos, M. *Science* **2003**, *301*, 935.
(11) Frindell, K. L. et al. Angew. Chem., Int. Ed. **2002**, *41* (6), 959.
(12) Yan, W.; Chen, B.; Mahurin, S. M.; Schwartz, V.; Mullins, D. R.; Lupini, A.; Pennycook, S. J.; Dai, S.; Overbury, S. H. **2004**, submitted.
(13) Huang, W.; Tang, X.; Wang, Y.; Koltypin, Y.; Gedanken, A. *Chem. Commun.* **2000** 1415.
(14) Zheng, Y.; Shi, E.; Cui, S.; Li, W.; Hu, X. *J. Mater. Sci. Lett.* **2000**, *19*, 1445.
(15) Reactor system borrowed from Bare, S. R. (UOP). Experimental details to be published in *Rev. Sci. Instrum.*
(16) Vaarkamp, M.; Linders, J. C.; Koningsberger, D. C. *Physica B* **1995,** *209*, 159.
(17) Cook, J. W.; Sayers, D. E. *Solid State Ionics* **1985**, *16*, 23.
(18) Clause, O.; Kermarec, M.; Bonneviot, L.; Villain, F.; Che, M. *J. Am. Chem. Soc.* **1992**, *114*, 4709.
(19) Ankudinov, A. L.; Rehr, J. J. *Phys. Rev. B* **1997**, *56*, 1712.
(20) Salama, T. M.; Shido, T.; Ohnishi, R.; Ichikawa, M. *J. Phys. Chem.* **1996**, *100*, 3688.
(21) Frenkel, A. I.; Hills, C. W.; Nuzzo, R. G. *J. Phys. Chem. B* **2001**, *105* (51), 12690.
(22) Jentys, A. *Phys. Chem. Chem. Phys.* **1999**, *1*, 4059.
(23) De Graaf, J.; van Dillen, J.; de Jong, K. P.; Koningsberger, D. C. *J. Catal.* **2001**, *203*, 307.
(24) Zanella, R.; Giorgio, S.; Henry, C. R.; Louis, C. *J. Phys. Chem. B* **2002**, *106*, 7634.
(25) Lee, S. J.; Gavriilidis, A. *J. Catal.* **2002**, *206*, 305.
(26) Englisch, M.; Lercher, J. A.; Haller, G. L. In *X-Ray Absorption Fine Structure for Catalysis and Surfaces*; Iwasawa, Y., Ed.; World Scientific: 1996; p 276.
(27) Vaarkamp, M.; Miller, J. T.; Modica, F. S.; Lane, G. S.; Koningsberger, D. C. In *Proc. 10th Intern. Congr. Catal.* Guczi, L., Solymosi, F., Tétényi, Eds.; Elsevier Sci. Pub.: 1993; Vol. A, 809.
(28) Sanchez, R. M. T.; Ueda, A.; Tanaka, K.; Haruta, M. *J. Catal.* **1997**, *168*, 125.
(29) Haruta, M. *CATTECH* **2002**, *6*, 102..
(30) Costello, C. K.; Kung, M. C.; Oh, H.-S.; Wang, Y.; Kung, H. H. *Appl. Catal., A* **2002**, *232*, 159.
(31) Costello, C. K.; Yang, J. H.; Law, H. Y.; Wang, Y.; Lin, J. N.; Marks, L. D.; Kung, M. C.; Kung, H. H. *Appl. Catal., A* **2003**, *243*, 15.
(32) Fritsche, H.-G.; Büttner, T. *Z. Phys. Chem.* **1999**, *209*, 93.
(33) Yan, W.; Chen, B.; Mahurin, S. M.; Dai, S.; Overbury, S. H. *Chem. Commun.* **2004**, in press.